

## High precision dynamic alignment and gap control for optical near-field nanolithography

Xiaolei Wen, Luis M. Traverso, Pornsak Srisungsitthisunti, Xianfan Xu, and Euclid E. Moon

Citation: *J. Vac. Sci. Technol. B* **31**, 041601 (2013); doi: 10.1116/1.4809519

View online: <http://dx.doi.org/10.1116/1.4809519>

View Table of Contents: <http://avspublications.org/resource/1/JVTBD9/v31/i4>

Published by the AVS: Science & Technology of Materials, Interfaces, and Processing

---

### Additional information on *J. Vac. Sci. Technol. B*

Journal Homepage: <http://avspublications.org/jvstb>

Journal Information: [http://avspublications.org/jvstb/about/about\\_the\\_journal](http://avspublications.org/jvstb/about/about_the_journal)

Top downloads: [http://avspublications.org/jvstb/top\\_20\\_most\\_downloaded](http://avspublications.org/jvstb/top_20_most_downloaded)

Information for Authors: [http://avspublications.org/jvstb/authors/information\\_for\\_contributors](http://avspublications.org/jvstb/authors/information_for_contributors)

## ADVERTISEMENT

# Instruments for advanced science

**Gas Analysis**



- dynamic measurement of reaction gas streams
- catalysis and thermal analysis
- molecular beam studies
- dissolved species probes
- fermentation, environmental and ecological studies

**Surface Science**



- UHV TPD
- SIMS
- end point detection in ion beam etch
- elemental imaging - surface mapping

**Plasma Diagnostics**



- plasma source characterization
- etch and deposition process reaction kinetic studies
- analysis of neutral and radical species

**Vacuum Analysis**




- partial pressure measurement and control of process gases
- reactive sputter process control
- vacuum diagnostics
- vacuum coating process monitoring

contact Hiden Analytical for further details

**HIDEN ANALYTICAL**

[info@hideninc.com](mailto:info@hideninc.com)  
[www.HidenAnalytical.com](http://www.HidenAnalytical.com)

CLICK to view our product catalogue 

# High precision dynamic alignment and gap control for optical near-field nanolithography

Xiaolei Wen

School of Mechanical Engineering and Birck Nanotechnology Center, Purdue University, West Lafayette, Indiana 47906 and Department of Optics and Optical Engineering, the University of Science and Technology of China, Hefei, Anhui 230026, China

Luis M. Traverso, Pornsak Srisungsitthisunti,<sup>a)</sup> and Xianfan Xu<sup>b)</sup>

School of Mechanical Engineering and Birck Nanotechnology Center, Purdue University, West Lafayette, Indiana 47906

Euclid E. Moon

Department of Electrical Engineering and Computer Science, Massachusetts Institute of Technology, Cambridge, Massachusetts 02139

(Received 11 February 2013; accepted 21 May 2013; published 6 June 2013)

The authors demonstrate the use of interferometric-spatial-phase-imaging (ISPI) to control a gap distance of the order of nanometers for parallel optical near-field nanolithography. In optical near-field nanolithography, the distance between the optical mask and the substrate needs to be controlled within tens of nanometers or less. The ISPI technique creates interference fringes from checkerboard gratings fabricated on the optical mask, which are used to determine the gap distance between the mask and the substrate surfaces. The sensitive of this gapping technique can reach 0.15 nm. With the use of ISPI and a dynamic feedback control system, the authors can precisely align the mask and the substrate and keep variation of the gap distance below 6 nm to realize parallel nanolithography. © 2013 American Vacuum Society. [<http://dx.doi.org/10.1116/1.4809519>]

## I. INTRODUCTION

Nanofabrication technologies play important roles in the progress of nanoscience and nanotechnology. Among various nanofabrication methods, optical near-field nanolithography using near-field optical focusing elements has great potentials due to its low-cost and possibility of parallel operation.<sup>1,2</sup> However, radiation from the exit-plane of near-field optical elements is only collimated within tens of nanometers, beyond which it diverges and its intensity decreases significantly.<sup>2-4</sup> Thus, a precise control over the separation distance between the near-field optical elements and the photoresist-coated surface is a great challenge to realize optical near-field nanolithography.<sup>1,3,5,6</sup> Srituravanich *et al.* utilized the computer hard disk air-bearing slider technique to obtain a nanoscale gap in thermal lithography.<sup>7</sup> Kim *et al.* reported integrating a solid immersion lens with a metallic sharp-ridged nanoaperture and using a gap error signal from evanescent coupling within the air-gap to realize sub-100 nm nanolithography.<sup>8</sup>

In this work, a gap-control system named interferometric-spatial-phase-imaging (ISPI) is utilized for real-time feedback in a near-field optical nanolithography system. The ISPI gapping is based on the detection of interference fringes from a set of specially designed gratings on an optical mask.<sup>9-12</sup> By analyzing interference signals, the frequency and phase information of the interference fringes can be obtained and used to derive the value of the gap between the mask and the substrate. The ISPI system employs oblique

light incident geometry so that it can be integrated with the lithography system without interfering with the lithography process. In theory, the ISPI gratings can be designed for an arbitrarily gap range.<sup>13</sup> For example, it has been used for gaps of tens of micrometers for parallel zone plate array lithography<sup>12,14</sup> and materials growth.<sup>15</sup> In this work, we demonstrate using ISPI to control a gap less than 20 nm for near-field optical nanolithography with sensitivity in the subnanometer lever. Moreover, we demonstrate real-time detection and feedback control of the gap during the nanolithography process. Therefore, with the use of ISPI, we can align the optical mask and the photoresist substrate to a high degree of parallelism and dynamically control the gap during the lithography process, and to realize parallel nanopatterning and move toward scalable parallel lithography. We demonstrate parallel lithography results using a 5×5 array of bowtie aperture antennas as focusing elements, which produce feature line-width below 90 nm.

## II. EXPERIMENTAL DETAILS

The experimental setup of the near-field optical lithography system consists of two subsystems as shown in Fig. 1: the lithography system and the ISPI system. In the lithography system, bowtie aperture antennas are chosen as the focusing element due to their ability of field localization and enhancement at the nanometer scale.<sup>3-5,16</sup> A bowtie aperture antenna is illustrated in Fig. 2(a). When the incident light is polarized across the gap (along the y-direction), a current is induced in the antenna and flows toward and concentrates at the tips at the gap, which produces an optical spot as small as the gap [Fig. 2(b)]. This near-field optical spot, on the other hand, is subjected to strong divergence. For example, a

<sup>a)</sup>Present address: Production Engineering Department, King Mongkut's University of Technology North Bangkok, Bangkok 10800, Thailand.

<sup>b)</sup>Electronic mail: [xxu@ecn.purdue.edu](mailto:xxu@ecn.purdue.edu)

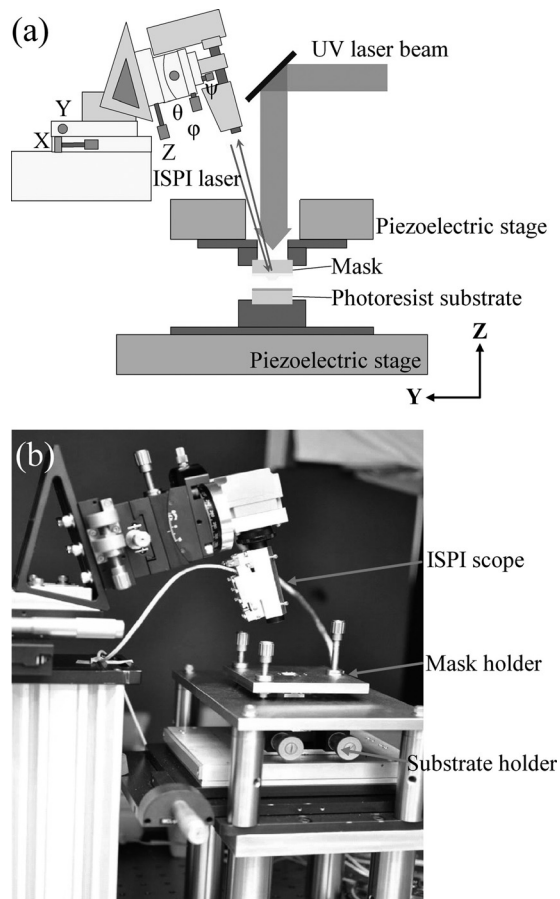


FIG. 1. (a) Illustration of the experimental setup; (b) photo of the experimental setup.

spot of 50 nm can double its size at a distance 50 nm from the antenna and its intensity also drops rapidly. Therefore, the effective working distance of a bowtie aperture antenna during a lithography process is well below 50 nm.

The ISPI gap detection is based on the analysis of fringes produced by light diffraction off chirped gratings referred to as transverse chirp gapping.<sup>10</sup> As shown in Fig. 3(a), the ISPI grating pattern consists of a pair of two dimensional checkerboards, whose y-periodicity is uniform and the x-periodicity is chirped oppositely. The y-periodicity is designed for oblique angle to avoid interfering with the lithography processing beam. The x-periodicity creates interference fringes that are sensitive to the mask–substrate gap. Since the x-periodicity is chirped, the transmitted-diffracted angle of the incident beam will vary along the x-direction as shown in Fig. 3(b). After reflecting from the substrate, the transmitted-diffracted beam will reach the mask some distance away from the incident position and rediffract. All the re-diffracted beams will then interfere and display a set of interference fringes at the imaging plane of the ISPI microscope as shown in Fig. 3(a). The position and number of the fringes are sensitive to the gap distance. When the gap is changed, the two sets of fringes will translate oppositely along the x-axis due to the counter chirped direction of the two checkerboard gratings. By analyzing the interference signal, we can extract the frequency (i.e., the number of the

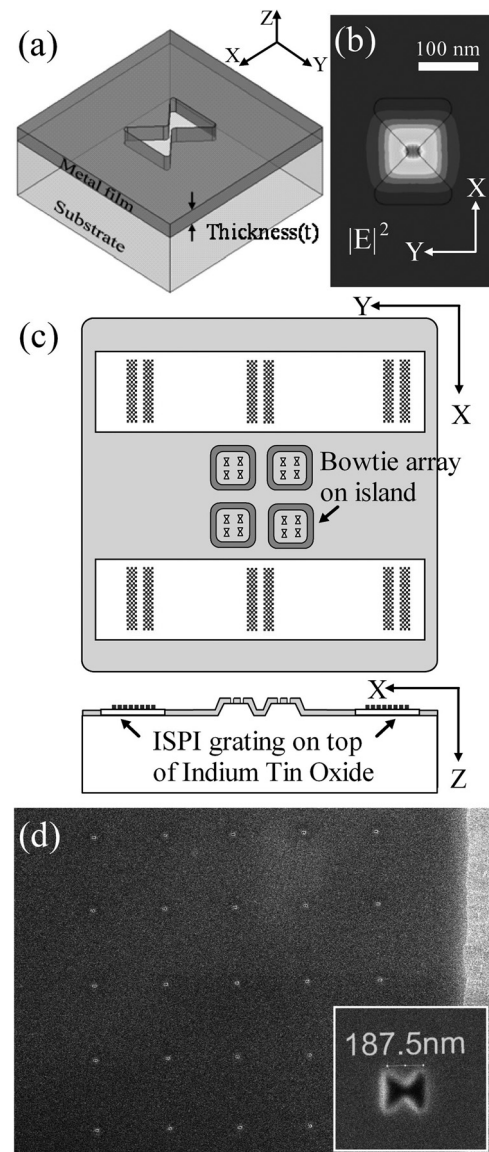


FIG. 2. (a) Sketch of the bowtie aperture, (b) its optical transmission intensity at the exit plane, (c) sketch of the mask, and (d) SEM image of a bowtie array on top of one island (the inset is a zoom-in image of one of the bowtie apertures).

fringes shown in the x-direction) and the relative phase shift of the two opposite fringes, and then derive the gap value from such information.

Figure 2(c) illustrates the optical mask, which was fabricated on a piece of 0.5 in. square optically flat quartz covered by a 70-nm layer of chromium. It contains several sets (six shown) of ISPI patterns and a number of islands (four shown). The bowtie apertures were milled on top of the island using focused ion beam milling [Fig. 2(d)]. The use of the islands can reduce the contact area between the mask and the photoresist (S1805, from Shipley) surfaces, so as to reduce the probability of contamination from dust particles. An SEM image of the bowtie apertures is shown in Fig. 2(d).

To implement the ISPI system, its microscope is mounted at an oblique angle above the lithography system using a 6-axis manually controlled stage so that it can be alternated to

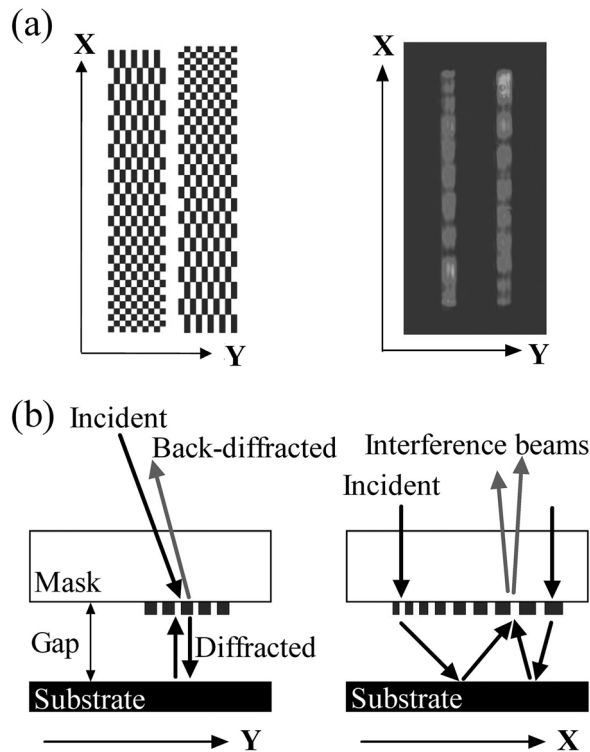


Fig. 3. (a) Sketch of ISPI checkerboard gratings and typical fringe image captured by the ISPI camera. (b) Illustration of the working mechanism of ISPI.

different ISPI grating patterns on the mask during the alignment process. A fiber laser with a 660 nm wavelength is attached to the microscope. It incidents onto the ISPI patterns, diffracts through the gap between the mask and substrate, and then reflects back to the microscope. The angle between the incident beam and the reflect beam is set to  $\sim 4^\circ$ .

The lithography process utilizes a frequency-tripled diode-pumped solid state UV laser ( $\lambda = 355$  nm) as the exposure source. To ensure the uniformity of the exposure dose on the entire bowtie aperture array for parallel lithography, the laser beam is expanded to cover an area of about  $2 \text{ cm}^2$ . The substrate is held by a piezoelectric stage, which can move in x-, y-, and z-directions with a 0.4 nm resolution. Above the substrate, the mask is held by another piezoelectric stage which can adjust the tip/tilt angles ( $\theta_x, \theta_y$ ) for alignment. The entire setup is built inside a cleanroom-grade semiclosed box to minimize contamination from dust particles.

### III. RESULTS AND DISCUSSION

#### A. Gap detection and control using ISPI

In our work, the ISPI pattern along the x-direction was designed to be chirped as a quartic function so that the frequency of the fringes would change linearly with the gap as shown in the simulation result [Fig. 4(a), square dots]. When an ISPI fringe image is obtained and its frequency and phase information is analyzed, the gap value can then be obtained using a calibrated linear equation. Figure 4(b) shows the

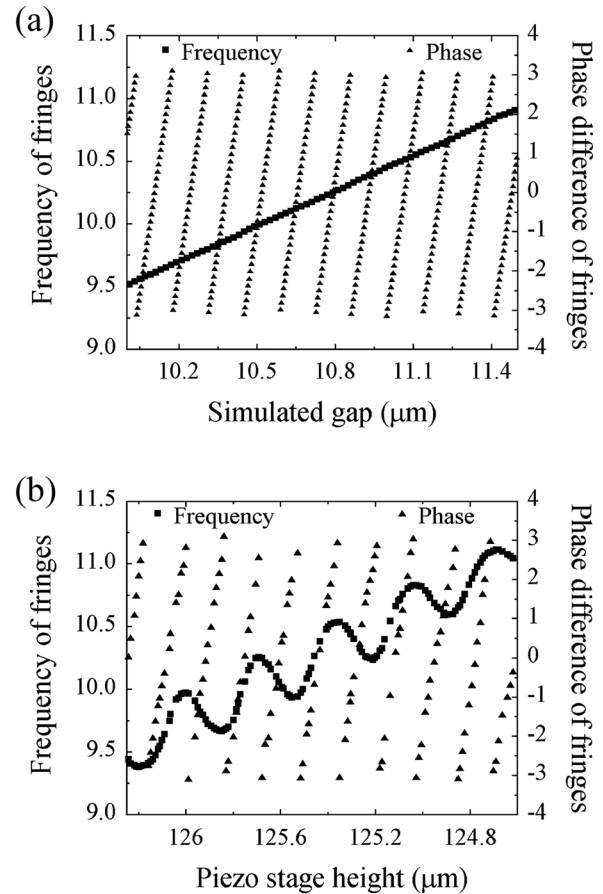


Fig. 4. (a) Simulated and (b) experimental relation of the frequency and phase of the fringes vs the gap.

change of the experimental data with the height of the piezoelectric stage. Since the position of the mask is fixed, when the height of the piezoelectric stage is increased, the gap between the mask and the substrate is decreased. From the experimental data, the frequency signal shows oscillations superimposed on the predicted linear trend. These oscillations are due to Fabry–Perot interference within the gap. On the other hand, the phase signal does not have any oscillation. Therefore, using the phase signal to determine the gap is more reliable than frequency gapping. From calibration, one phase cycle ( $2\pi$ ) corresponds to about 150 nm of gap change. The detection algorithm in our system is capable to detect  $< 1/1000$  of a phase cycle; thus, the sensitivity of phase gapping is 0.15 nm (150 nm/1000).

We also implemented a real-time feedback control system to maintain the gap distance. Figures 5(a) and 5(b) illustrate gapping with and without the feedback control. When there is no feedback, the gap drifts for hundreds of nanometers even when the piezoelectric stage is not moving, which can be caused by the background noises from the vibration of the piezoelectric stage or thermal expansion. With the feedback control, the gap can remain at the desired value within about 4 nm. When the piezoelectric stage moves, Fig. 5(c) shows variation of the gap distance is about 40 nm over a scanning distance of  $100 \mu\text{m}$  without the feedback control, which can be caused by a small tip–tilt angle from misalignment. When

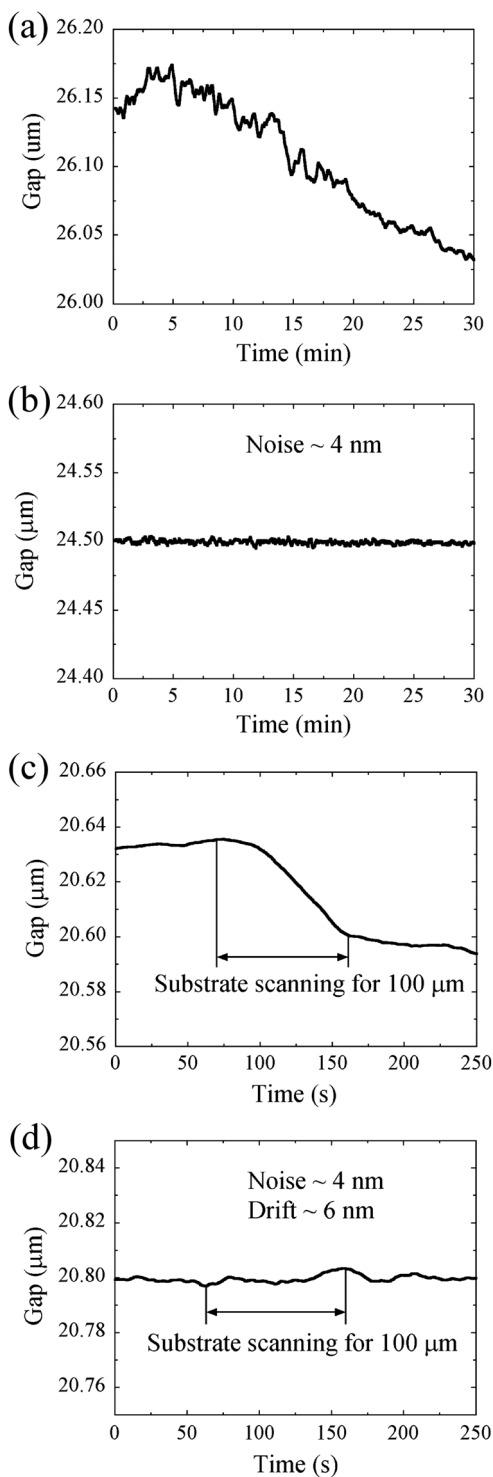


FIG. 5. ISPI gapping with and without feedback: (a) and (b) statically, and (c) and (d) during scanning.

the feedback control is activated, the variation of the gap distance is limited to 6 nm [Fig. 5(d)].

### B. ISPI alignment

As mentioned before, for near-field optical nanolithography, the alignment between the mask and the substrate is critical. For parallel lithography using multiple antennas, it

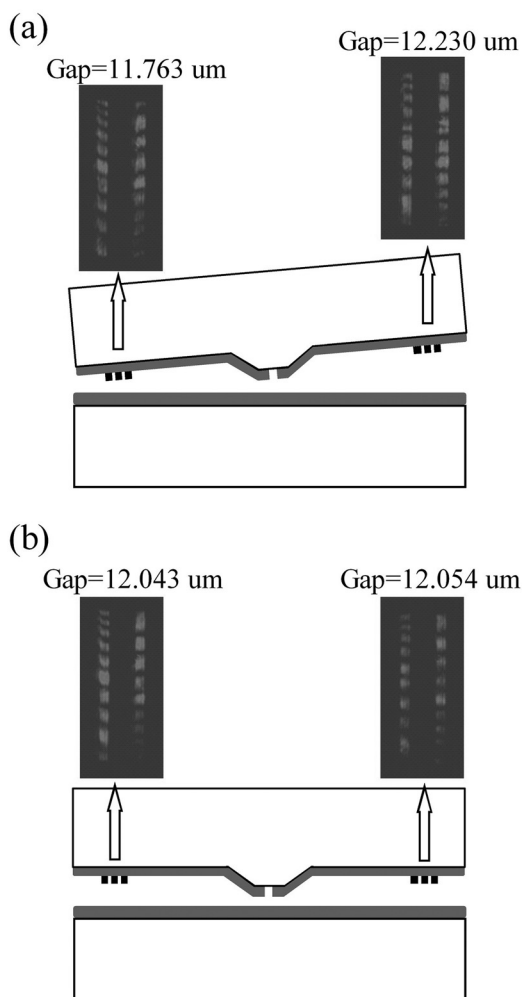


FIG. 6. Illustration of alignment using the ISPI detection: (a) before alignment; (b) after alignment.

is even more important to achieve a high degree of parallelism. We obtain gap values on different ISPI patterns on the mask [Fig. 2(c)] and then adjust the tip/tilt of the mask to make sure same gap values are obtained on different ISPI patterns and the mask is parallel to the substrate (Fig. 6). Typically, the process of reading the gap values and adjusting the tilt angles of the mask relative to the substrate needs to be repeated several times to achieve a parallelism within 0.03 mrad. To demonstrate parallel lithography, we use a 5×5 antenna array, which covers an area of 0.04 mm<sup>2</sup>. Within this area, a tilt of 0.03 mrad corresponds to a height difference of 6 nm.

### C. Parallel nanolithography

After aligning the mask parallel to the substrate (within 0.03 mrad), the photoresist substrate is brought into contact with the surface of the mask. The ISPI data are recorded when the substrate is moved toward the mask as shown in Fig. 7(a). It is seen that the gap decreases linearly when the substrate is moving toward the mask. Then there is a sudden turn of the slope of the gap reading, after which the gap

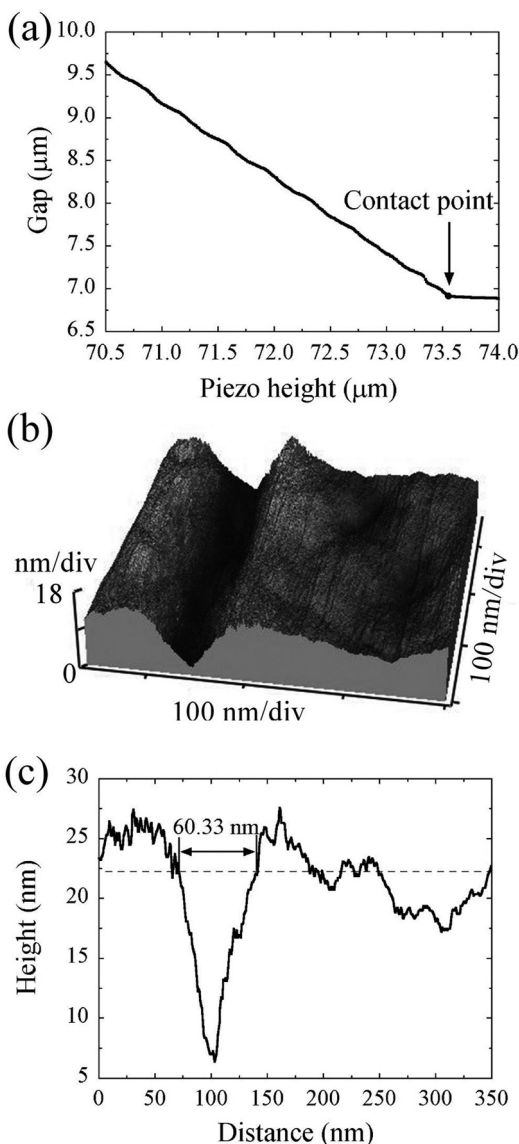


Fig. 7. (a) Height of the piezoelectric stage vs the gap value detected by the ISPI. (b) and (c) AFM results of the line produced with a speed of  $1.5 \mu\text{m/s}$  and a gap of 10 nm.

keeps a constant value. This indicates that the substrate has made a contact with the mask at the point when the slope changes. Therefore, from this contact point, the distance between the bowtie aperture antennas and the photoresist surface can be determined by retracting the substrate away from the mask. This provides a means to operate with a small gap to both minimize friction and maintain a gap distance within tens of nm for near-field nanolithography.

Figure 7(b) shows the lithography result with a gap distance of 10 nm and a scanning speed of  $1.5 \mu\text{m/s}$ , under a laser intensity of  $70 \text{ mW/cm}^2$ . The line-width is measured to be around 60 nm [Fig. 7(c)]. With the use of ISPI gapping and feedback control, we are able to achieve parallel nanolithography. Figure 8 shows the result of lithography using a  $5 \times 5$  bowtie aperture antenna array. The line-width of the features is about 86 nm. The small variations among different patterns are due to the difference among the bowtie aperture antennas caused by the fabrication process.

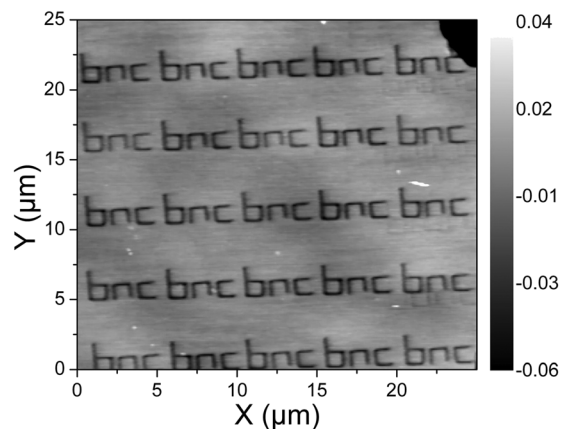


Fig. 8. Result of parallel lithography with a line width of 86 nm.

#### IV. CONCLUSIONS

We demonstrated the ISPI gapping technique in parallel nanolithography, using bowtie aperture antennas as near field optical elements. With the use of ISPI phase gapping, the sensitivity of gap detection can reach 0.15 nm. Combining ISPI and dynamic feedback control, we can precisely align the mask with the substrate with a parallelism better than 0.03 mrad, and then control the gap between the mask and the substrate during nanolithography with a variation less than 6 nm, which offers a means to realize parallel nanolithography.

#### ACKNOWLEDGMENTS

Support to this work by the Defense Advanced Research Projects Agency (Grant No. N66001-08-1-2037) and the National Science Foundation (Grant No. CMMI-1120577) are gratefully acknowledged. X.W. also acknowledge the support from the National Basic Research Program (973 Program) of China under Grant No. 2013CBA01703.

- <sup>1</sup>S. M. V. Uppuluri, E. C. Kinzel, Y. Li, and X. Xu, *Opt. Express* **18**, 7369 (2010).
- <sup>2</sup>P. Srisungsitthisunti, O. K. Ersoy, and X. Xu, *Appl. Phys. Lett.* **98**, 223106 (2011).
- <sup>3</sup>E. X. Jin and X. Xu, *Jpn. J. Appl. Phys.* **43**, 407 (2004).
- <sup>4</sup>E. X. Jin and X. Xu, *Appl. Phys. Lett.* **86**, 111106 (2005).
- <sup>5</sup>N. Murphy-DuBay, L. Wang, and X. Xu, *Appl. Phys. A* **93**, 881 (2008).
- <sup>6</sup>H. Hwang, J.-G. Kim, K. W. Song, K.-S. Park, N.-C. Park, H. Yang, Y.-C. Rhim, and Y.-P. Park, *Jpn. J. Appl. Phys.* **50**, 09MC04 (2011).
- <sup>7</sup>W. Srituravanich, L. Pan, Y. Wang, C. Sun, D. B. Bogy, and X. Zhang, *Nat. Nanotechnology* **3**, 733 (2008).
- <sup>8</sup>T. Kim *et al.*, *Appl. Phys. Lett.* **101**, 161109 (2012).
- <sup>9</sup>E. E. Moon, P. N. Everett, M. W. Meinhold, M. K. Mondol, and H. I. Smith, *J. Vac. Sci. Technol. B* **17**, 2698 (1999).
- <sup>10</sup>E. E. Moon and H. I. Smith, *J. Vac. Sci. Technol. B* **24**, 3083 (2006).
- <sup>11</sup>E. E. Moon, P. N. Everett, M. W. Meinhold, and H. I. Smith, *Proceedings of Microprocesses and Nanotechnology Conference* (IEEE, New York, 2000), p. 252.
- <sup>12</sup>P. Srisungsitthisunti, E. E. Moon, C. Tansarawiput, H. Zhang, M. Qi, and X. Xu, *Proc. SPIE* **7767**, 776707 (2010).
- <sup>13</sup>P. Srisungsitthisunti, Ph.D. dissertation (Purdue University, 2011).
- <sup>14</sup>R. Menon, E. E. Moon, M. K. Mondol, F. J. Castano, and H. I. Smith, *J. Vac. Sci. Technol. B* **22**, 3382 (2004).
- <sup>15</sup>J. I. Mitchell, S. J. Park, C. A. Watson, P. Srisungsitthisunti, C. Tansarawiput, M. S. Qi, A. Eric, C. Yang, and X. Xu, *Opt. Eng.* **50**, 104301 (2011).
- <sup>16</sup>L. Wang, S. M. Uppuluri, E. X. Jin, and X. Xu, *Nano Lett.* **6**, 361 (2006).